

Approaches to Calculation of Exciton Interaction Energies for a Molecular Dimer

I. A. Howard,^{*,†} F. Zutterman,[‡] G. Deroover,[‡] D. Lamoen,[†] and C. Van Alsenoy[§]

Department of Physics, University of Antwerp, Groenenborgerlaan 171, B-2020 Antwerp, Belgium, Agfa-Gevaert N.V., Septestraat 27, B-2640 Mortsels, Belgium, and Department of Chemistry, University of Antwerp, Universiteitsplein 1, B-2610 Antwerp, Belgium

Received: June 7, 2004; In Final Form: September 23, 2004

For two model systems, a dimer of *N,N'*-dimethyl thiacyanocyanine and a dimer of C.I. Pigment Yellow 12, we compare results of several approaches to calculation of the exciton interaction energy. The sum over Coulombic interactions between atomic transition charges is compared to the point-dipole and extended-dipole approximations and to the direct evaluation of the Coulomb interaction integral over transition charge densities, for a range of dimer configurations. Calculations are carried out at semiempirical, *ab initio* Hartree–Fock, and *ab initio* configuration interaction—singles levels. Finally, we discuss the relation of these interaction energies to those calculated using a supermolecular approach. We conclude that for the materials studied, semiempirical methods are adequate to describe the excitonic shift.

I. Introduction

The calculation of the exciton interaction energy is a matter of importance in describing photoexcitations in a number of materials of current interest. Dyes and pigments are widely used in practical applications, particularly in printing and imaging technology. New dyes and pigments with improved properties need to be constantly developed. Rational design of such materials requires the accurate prediction of their electronic excitations in the visible range of the spectrum. In practice pigments are always used in crystalline form, while dyes, which are soluble, are often used in the form of two-dimensional aggregates on crystal surfaces (e.g., AgX). Stacking dye or pigment molecules in two- or three-dimensional arrays often results in an optical spectrum that strongly differs from the spectrum of the dissolved molecule. No well-validated first-principles methods currently exist for the prediction of photoexcitations in molecular crystals, though there is steady progress toward this goal. For example, the electronic and optical properties of solid pentacene were recently predicted with good accuracy using the GW-BSE method.¹

Pending the development of a generally valid first-principles method, one has to resort to the approximation provided by Frenkel exciton theory.² Molecules of dyes or pigments frequently have a single electronic transition of high oscillator strength in the visible spectrum (ignoring vibrational replicas). The high oscillator strength results in strong excitonic coupling in molecular aggregates and crystals, which in turn has a strong impact on the excitation energy in these systems. Exciton coupling is only one of the reasons that the excitation energy in an aggregate or crystal is different from that in an isolated monomer.^{3,4} The contribution exciton coupling makes to the shift of the excitation energy may be called the “exciton shift”; another contribution is the so-called gas-to-crystal shift.⁵ This is the shift of the on-site excitation energy caused by the fact

that a ground-state molecule and an excited-state molecule interact differently by van der Waals, electrostatic, and hydrogen-bonding interactions than two ground-state molecules. Additional contributions to the shift may be due to configurational mixing with higher-energy excitations;^{6,7} particularly important at short intermolecular distances is the influence of charge-transfer excitations.^{8–10} In aggregates and crystals of dye or pigment molecules the exciton shift is often the predominant contribution to the spectral shift. In searching for a practical method for predicting excitation energies in such systems, accurate prediction of the exciton shift is of particular interest.

In the infinite-size approximation the exciton shift in a crystal or aggregate having one molecule in the asymmetric unit (the simplest case) is calculated by summation of all exciton interaction energies between a reference molecule and all other molecules. The optically allowed excitation is found at the $k = 0$ limit by selecting an all-in-phase relationship of the transition charge densities on the molecules. Since calculation of the exciton shift in a molecular crystal or aggregate involves a summation of pairwise intermolecular contributions, the accuracy of the calculation depends on how accurately the exciton shift can be calculated for a dimer. The exciton shift in a dimer can be calculated in several ways. Ideally, true wave functions of the dimer are calculated, for example by an SCF calculation followed by a configuration interaction treatment (e.g., configuration interaction—singles, CIS). In a dimer intermolecular interactions generally split any excited state of an isolated monomer into two excited states with different energies and transition dipole moments. If effects due to configurational mixing of charge-transfer states and higher-lying molecular excited states can be ignored, the exciton shift is then equal to half the difference between the two excitation energies (this is the “supermolecule” approach discussed in section IV). However, for the calculation of exciton shifts in a crystal or aggregate the supermolecule approach is not practical. Indeed, the number of exciton interactions that needs to be taken into account is theoretically infinite for an infinite crystal. In practice interactions with molecules further away from the reference molecule

[†] Department of Physics, University of Antwerp.

[‡] Agfa-Gevaert N.V.

[§] Department of Chemistry, University of Antwerp.

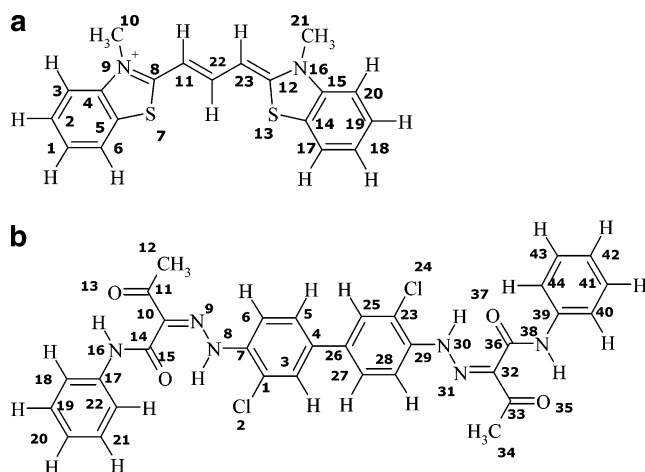


Figure 1. (a) Cyanine monomer; (b) PY 12 monomer. Atom numbers correspond to those in Tables 1 and 2. Hydrogens are not numbered.

than a cutoff value can be ignored. Due to the long range of the exciton interactions, which are Coulomb interactions, the cutoff limit can be as large as 10 nm (depending on the accuracy aimed for). Consequently, the number of pairwise exciton shifts that need to be summed up to give the exciton shift in the crystal is typically very large. It is therefore of interest to search for the simplest possible method for calculating exciton shifts in dimers that is sufficiently accurate for the purpose of dye or pigment design. This is the purpose of the work reported here.

Within the framework of Frenkel exciton theory the dimer wave functions are assumed to be built from unperturbed molecular wave functions. The exciton shift is equal to first order (assuming exact molecular wave functions are available, and neglecting exchange contributions) to the Coulomb interaction energy between the transition charge densities on the two molecules. The optimum procedure for calculation of the exciton shift, or exciton interaction energy, is dependent partially on the material in question and partially on the degree of computational effort involved. In several recent papers a number of approaches have been compared for conjugated polymers, based on ZINDO treatments.^{11,12} Here, we consider instead exciton interaction energies in a molecular aggregate or crystal and compare, for two model systems of molecular dimers, five approaches to evaluation of the exciton interaction energy: the point-dipole approximation, the extended-dipole approximation, the sum over Coulombic transition charge interactions, the direct evaluation of the Coulomb interaction integrated over transition charge densities, and the supermolecular approach. Results from semiempirical ZINDO are compared with those from ab initio Hartree–Fock (HF) and ab initio CIS.

II. Computational Methods and Model Systems

We consider as our first model system the dimer of *N,N'*-dimethyl thiocarbocyanine, hereafter referred to simply as the cyanine dimer. Aggregates of analogues of this molecule are extensively used as spectral sensitizers in color photography. The monomer, shown in Figure 1a, is taken to be planar except for the methyl group hydrogens, with a “length” of approximately 15 Å. Geometry of the (cationic) monomer was optimized using DMol³ with the BP nonlocal functional and the DNP basis set.¹³ The second model system considered is a dimer of a considerably more extended molecule, C.I. Pigment Yellow 12 (PY 12); the monomer is shown in Figure 1b. PY 12 and its analogues are widely used as colorants in inks and paints. As we will see in section III, these two systems have

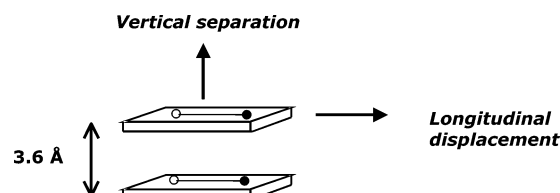


Figure 2. Schematic illustration of the two displacement paths considered for the cyanine dimer and the PY 12 dimer.

quite different distributions of transition charge, allowing us to test the general validity of the calculational methods considered. In both sets of dimers, we initially consider the monomers to be vertically stacked (i.e., one molecule is translated relative to the other in a direction perpendicular to the chromophore plane: see Figure 2). As mentioned above, a range of calculational methods has been used: semiempirical ZINDO,¹⁴ ab initio HF, and ab initio CIS. In the semiempirical calculations we used the ZINDO implementation with the INDO/1 Hamiltonian in the Cerius² modeling environment from Accelrys. A CIS space of 10 orbitals above and below the highest occupied orbital has been taken in calculations involving a monomer, and 20 orbitals above and below the highest occupied for dimer (supermolecular) calculations. For the ab initio HF and CIS approaches, as well as for the subsequent charge partitioning, we have employed the Hartree–Fock MIA method as implemented in the BRABO code.¹⁵ In all HF and CIS calculations, the 6-31G** basis has been used. The ab initio CIS calculations, using the HF ground state as reference, were carried out within a space of 10 orbitals above and 10 below the highest occupied level. We consider only singlet excitations, as triplet excitations have zero associated oscillator strength.

III. Exciton Interaction Energy

The exciton interaction energy is a measure of the splitting of the excited state of the dimer by the intermolecular interaction Hamiltonian. In the standard exciton theory for the dimer, this interaction energy ΔE can be evaluated as the Coulomb interaction energy between the two transition charge densities $\rho_1^T(\mathbf{r}_1)$ and $\rho_2^T(\mathbf{r}_2)$ centered on the dimer molecules 1 and 2, i.e.,

$$\Delta E = \int_{\mathbf{r}_2} \int_{\mathbf{r}_1} \frac{\rho_1^T(\mathbf{r}_1) \rho_2^T(\mathbf{r}_2)}{|\mathbf{r}_1 - \mathbf{r}_2|} d\mathbf{r}_1 d\mathbf{r}_2 \quad (1)$$

(Here, and subsequently, atomic units are used.) The transition charge density $\rho^T(\mathbf{r}) = \sum_{\mu\lambda} P_{\mu\lambda} \phi_\mu(\mathbf{r}) \phi_\lambda^*(\mathbf{r})$ is that of an isolated monomer, on the assumption of weakly interacting monomers (an assumption largely valid in molecular crystals). Here, μ and λ sum over all basis functions $\phi_\mu(\mathbf{r})$, $\phi_\lambda(\mathbf{r})$, while $P_{\mu\lambda} = \sum_o \sum_v C_{ov} c_{\mu o} c_{\lambda v}^*$, where the $c_{\mu o}$ and $c_{\lambda v}$ are the coefficients describing the occupied and virtual molecular orbitals, respectively, and the C_{ov} describe the excitation from occupied orbital o to virtual orbital v . We have neglected dielectric screening, since we are dealing with near-neighbor molecular dimers. There are several commonly used approximations to the interaction energy, ranging from the simple point-dipole model¹⁶ through the extended-dipole model¹⁷ to the summation over Coulombic interactions between the atomic transition charges on each atomic site.¹⁸ The point-dipole model, as was pointed out long ago,^{17,19} is valid only for dimer separations that are large compared to the molecular dimensions. In this model, interactions between extended transition charge densities are replaced by the interaction between the effective point (transition) dipoles μ of the monomers; the exciton interaction energy is then

approximated by the dipole–dipole interaction

$$\Delta E \cong \frac{\boldsymbol{\mu}_1 \cdot \boldsymbol{\mu}_2}{|\mathbf{r}_1 - \mathbf{r}_2|^3} - 3 \frac{[\boldsymbol{\mu}_1 \cdot (\mathbf{r}_1 - \mathbf{r}_2)][\boldsymbol{\mu}_2 \cdot (\mathbf{r}_1 - \mathbf{r}_2)]}{|\mathbf{r}_1 - \mathbf{r}_2|^5} \quad (2)$$

Despite its inaccuracy, this approximation is still frequently applied, even for molecules in close proximity.^{20–22} Somewhat more accurate is the extended-dipole model, in which the molecular transition charge density distribution is approximated by a dipole consisting of one single negative and one single positive charge (see Figure 2). The distribution of positive transition charge over the molecule can be used to determine a “center of mass” of the positive transition charge, and likewise for the negative transition charge. These two positions then determine the length and orientation of the monomeric dipole, with the effective charges—the sums respectively of all the positive and negative transition charges—placed at the ends of the dipole. The actual distribution of transition charge is still more precisely described by atomic transition charges q_i^T associated with each atomic site i . The exciton interaction energy is then approximated by the summation over Coulombic interactions between atomic transition charges on the two molecules:

$$\Delta E \cong \sum_{ij} \frac{q_i^T q_j^T}{|\mathbf{r}_{i_1} - \mathbf{r}_{j_2}|} \quad (3)$$

The summation over atomic transition charges gives a result that must depend to some degree of course on the method of charge partitioning applied to the density matrix. Below, we compare briefly the evaluation of atomic transition charges and consequent exciton interaction energies using Mulliken²³ and stockholder (Hirshfeld)²⁴ partitioning; elsewhere, we have used Mulliken partitioning exclusively. Preferable to any of these approximations, in principle, is of course a direct evaluation of ΔE from eq 1.

For the cyanine dimer the point-dipole approximation cannot be expected to be adequate except at separations greater than ~ 15 Å; for the PY 12 dimer, separations greater than ~ 25 Å would be necessary. As an illustration of this, we show in Figure 3 ZINDO results for the exciton interaction energy. Two displacement paths have been considered; the first corresponds to a vertical separation of the monomers, while along the second path the vertical separation is held at 3.6 Å, with relative displacements in the direction of the longitudinal axis of the molecule. These paths are shown schematically in Figure 2. Figure 3a displays ΔE as a function of vertical monomer separation in the cyanine dimer, calculated using point-dipole, extended-dipole, and atomic transition charge approximations. While the extended-dipole approximation is an improvement, it still differs considerably from the atomic transition charge results. An even more dramatic example is shown in Figure 3b, where the same approximations are compared for relative longitudinal displacement of the monomers in the PY 12 dimer, with the monomers held at a fixed vertical separation of 3.6 Å. The variation of the shift of the allowed excitation from positive to negative with displacement reproduces the well-known behavior in vertically stacked H-type versus longitudinally displaced J-type aggregates. Here both the point- and extended-dipole approximations are seen to be qualitatively inaccurate by as much as an order of magnitude. The severe failure of the extended dipole approximation in this case deserves some explanation. It appears to be due to the short length of the

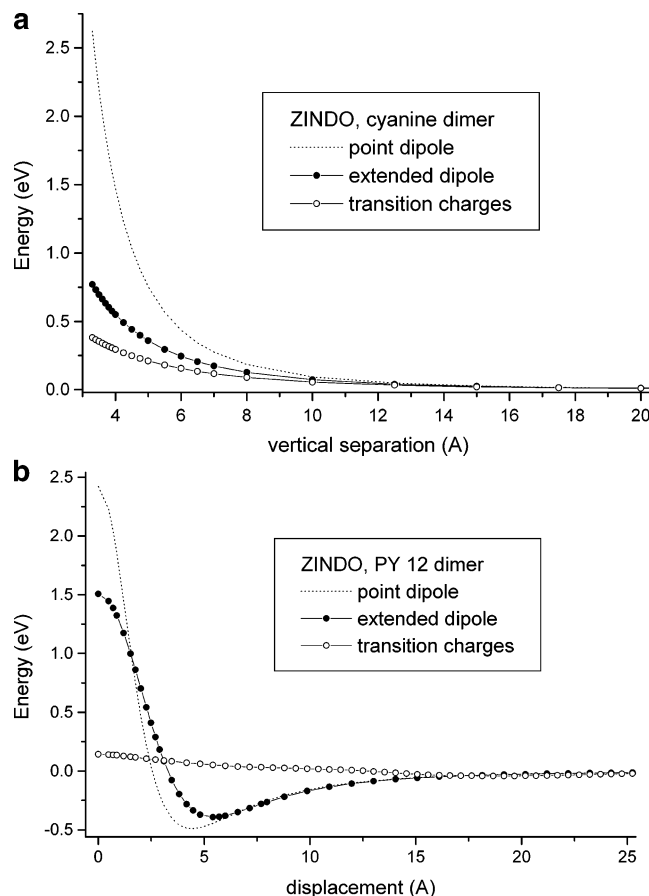


Figure 3. (a) ZINDO results for the exciton interaction energy ΔE of the cyanine dimer as a function of vertical monomer separation, calculated using point-dipole, extended-dipole, and transition charge approximations; (b) the same approximations compared for relative longitudinal slip of the monomers in the PY 12 dimer.

extended dipole (3.1 Å for PY12, compared to 6.3 Å for the cyanine), which makes it much more point-dipole-like than in the case of the cyanine. The large difference in extended-dipole lengths for the two molecules is a consequence of the quite different nature of their transition charge distributions, as can be seen in Tables 1 and 2 and as will be further discussed in section V.

We concentrate therefore on the summation over atomic transition charges in eq 3. For the cyanine and PY 12 monomers we have evaluated the (Mulliken) atomic transition charges at the ZINDO, HF, and CIS levels. (In the case of ZINDO the Mulliken partitioning formulas are adapted taking account of the fact that overlap between atomic orbitals is neglected.) In Table 1 we compare these results for the cyanine monomer. In addition, we compare the Mulliken and stockholder atomic transition charges for this monomer at the HF level. The differences, with few exceptions, are not large, and they do not result in a substantial difference in calculated exciton interaction energy. This latter point can be verified by using the charges of Table 1 in eq 3; for the cyanine dimer at 3.6 Å vertical separation, we find at the HF level an exciton interaction energy of 0.332 eV with Mulliken charges and 0.312 eV with stockholder charges. At 20 Å separation, interaction energies are 0.031 eV (Mulliken) and 0.030 eV (stockholder). Further comparison between ZINDO and ab initio results is carried out in section V. In Table 2 we compare the ZINDO and ab initio CIS Mulliken atomic transition charges for the PY 12 monomer. Again, the two approaches result in similar transition charge distributions.

TABLE 1: Atomic Transition Charges for the Cyanine Monomer at ZINDO (Mulliken), HF/6-31G (stockholder and Mulliken), and CIS/6-31G** (Mulliken) Levels^a**

atom no./ type	level of calculation			
	ZINDO	ab initio HF (stockholder)	ab initio HF (Mulliken)	ab initio CIS
1 C	0.052	0.027	0.034	0.055
2 C	0.011	0.012	0.010	0.019
3 C	0.018	0.012	0.015	0.021
4 C	-0.034	0.006	-0.005	-0.030
5 C	0.025	0.024	0.029	0.021
6 C	0.003	0.009	0.004	-0.002
7 S	0.044	0.073	0.075	0.100
8 C	0.054	0.046	0.052	0.043
9 N	0.134	0.060	0.072	0.075
10 C	0.000	0.008	0.000	0.000
11 C	0.025	0.047	0.055	0.024
12 C	-0.054	-0.047	-0.052	-0.043
13 S	-0.044	-0.073	-0.075	-0.100
14 C	-0.025	-0.023	-0.029	-0.021
15 C	0.034	-0.006	0.005	0.031
16 N	-0.134	-0.061	-0.072	-0.075
17 C	-0.003	-0.008	-0.004	0.002
18 C	-0.052	-0.027	-0.034	-0.055
19 C	-0.011	-0.012	-0.010	-0.019
20 C	-0.018	-0.011	-0.015	-0.021
21 C	0.000	-0.008	0.000	0.000
22C	0.000	0.000	0.000	0.000
23C	-0.025	-0.047	-0.055	-0.024

^a Hydrogen transition charges are negligible and are not listed. Atom numbering is as shown in Figure 1a.

Finally, for our two model dimers, we have evaluated eq 1 directly for a range of monomer separations. Results are discussed in section V. Our findings are in some contrast with results reported for dimers of a merocyanine that was treated at different levels of electron correlation.²⁵ In this earlier study the CIPSI method resulted in smaller transition charges (and, therefore, exciton interaction energies) than the CIS method. This suggests that the good correspondence we observed between results at the semiempirical and ab initio levels is a consequence of treating the electron correlation with the CIS method at both levels. We plan to study in future work if better treatment of the electron correlation can be implemented in a method that is practical for design of molecules of this size.

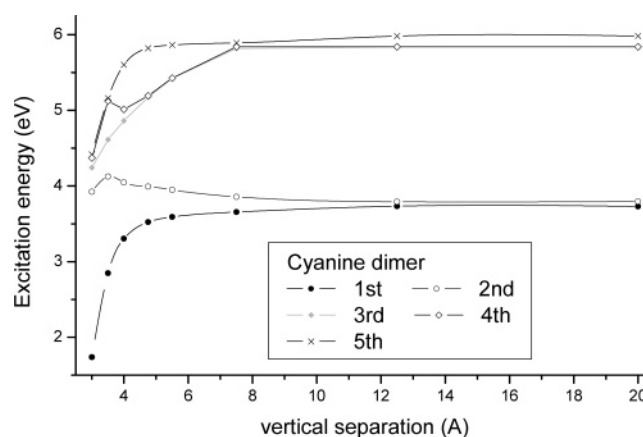
IV. Supermolecular Model

The exciton interaction energy as calculated from eq 1 does not include some aspects of the interaction between the monomers in a dimer. All aspects of the interaction are included, however, if we calculate the molecular orbitals for the dimer as a single entity, building the excited states then from these “delocalized” orbitals.^{26,27} In particular, there is the possibility of charge transfer between monomers, excluded in the evaluation of ΔE in eq 1 or eq 3. There is also the possibility of “mixing” of monomeric excited states. Furthermore, eq 1 does not take account of the gas-to-dimer shift (the equivalent of the gas-to-crystal shift in the dimer). We can take the effective interaction energy to be half the difference between first (E_1) and second (E_2) dimer excited-state energies, with the splitting between these states assumed to be due to the intermolecular interaction. For the displacements discussed in section III, we have calculated, using both ab initio CIS and ZINDO, the lowest excitation energies for the two model dimers. The CIS excitation energies are shown as a function of vertical separation for the cyanine dimer in Figure 4. As is well known, the CIS approach overestimates excitation energies, so the magnitudes of the

TABLE 2: Mulliken Atomic Transition Charges for the PY 12 Monomer at CIS/6-31G and ZINDO Levels^a**

atom no./type	ab initio CIS	ZINDO
1 C	-0.055	-0.048
2 Cl	-0.008	-0.002
3 C	0.084	0.044
4 C	-0.136	-0.123
5 C	0.070	0.042
6 C	-0.072	-0.050
7 C	0.136	0.115
8 N	-0.073	-0.105
9 N	-0.036	-0.047
10 C	0.117	0.156
11 C	0.019	0.014
12 C	0.000	0.001
13 O	0.040	0.038
14 C	0.001	0.003
15 O	0.005	0.017
16 N	0.017	0.017
17 C	-0.020	-0.019
18 C	0.006	0.004
19 C	-0.001	0.002
20 C	0.026	0.020
21 C	0.001	0.004
22 C	0.010	0.007
23 C	0.053	0.042
24 Cl	0.008	0.002
25 C	-0.085	-0.044
26 C	0.133	0.116
27 C	-0.069	-0.041
28 C	0.068	0.044
29 C	-0.135	-0.111
30 N	0.067	0.090
31 N	0.035	0.044
32 C	-0.109	-0.139
33 C	-0.018	-0.013
34 C	0.000	-0.001
35 O	-0.038	-0.034
36 C	0.000	-0.001
37 O	-0.005	-0.014
38 N	-0.016	-0.015
39 C	0.019	0.018
40 C	-0.005	-0.003
41 C	0.000	-0.002
42 C	-0.024	-0.019
43 C	-0.002	-0.003
44 C	-0.009	-0.006

^a Transition charges on hydrogens are negligible and therefore are not listed. Atoms are numbered as in Figure 1b.

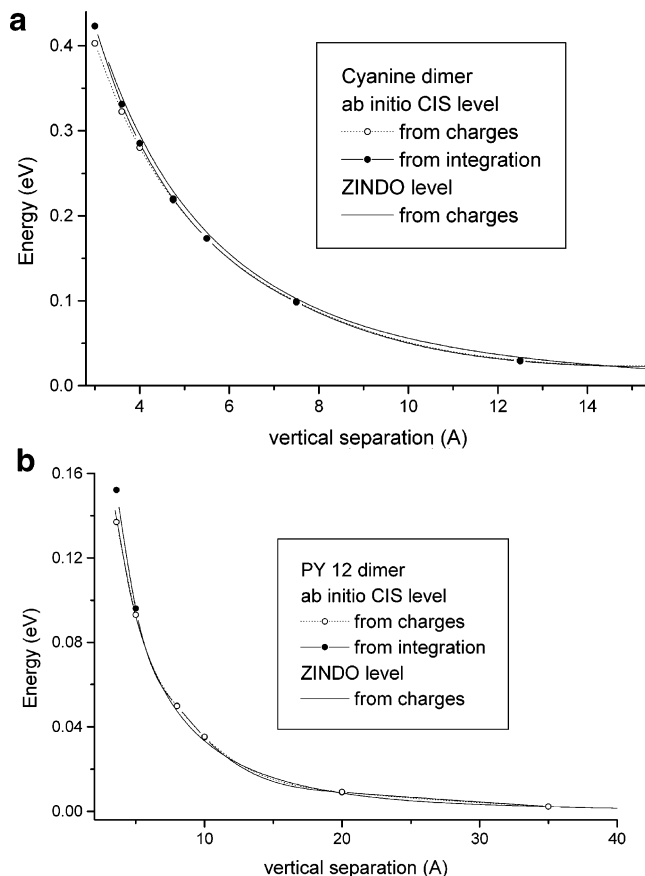
**Figure 4.** The lowest five CIS excitations, as a function of vertical separation, for the cyanine dimer.

energies in Figure 4 cannot be considered reliable; however, the variation of energies with monomer separation is the feature of interest here. In Figure 4, the first excitation (primarily involving the HF HOMO–LUMO pair) is seen to be well

TABLE 3: Transition Dipoles (in Debye) for the Three Lowest-Lying (singlet) Excitations in the Cyanine Dimer and Monomer

vertical displacement (Å)	excitation		
	1	2	3
Dimer			
3.5	0.003	17.282	0.585
4.0	0.001	17.023	0.451
4.75	0.003	16.999	0.319
5.5	0.004	16.993	0.160
7.5	0.001	17.094	0.003
12.5	0.002	17.163	0.010
20.0	0.002	17.159	0.010
Monomer			
	12.070	1.990	1.204

separated in energy from the second for small intermonomer distances; the first and second excitations approach each other above ~ 7 Å monomer separation, where they are nearly coincident, while the third through fifth also approach each other closely. At ~ 3 Å, however, there is a peak in the second excitation energy such that it closely approaches the third through fifth, which again are nearly coincident. The ZINDO evaluation of the lowest excitations gives very similar results. For monomer separations larger than 5 Å the first and second excitations can clearly be identified as the two almost pure Frenkel excitations derived from the lowest molecular excitation. For these same separations the third and fourth excitations are unambiguously identified as almost pure charge-transfer (CT) excitations from the HOMO of one molecule to the LUMO of the other. The nature of the fifth excitation was not investigated in detail. We suspect it to be predominantly one of the two Frenkel excitations derived from the second-lowest molecular excitation. This is confirmed by the fact that ab initio CIS places the second-lowest molecular excitation 2.1 eV above the lowest-energy one. This corresponds to the energy difference between the first/second and the fifth excitation in the dimer at large separation. It should be pointed out that for separations larger than 7 Å ZINDO places the CT excitations largely above the Frenkel excitations derived from the second-lowest molecular excitation, while ab initio CIS places them at nearly the same energy. Ab initio CIS apparently exaggerates the CT excitation energies less than the molecular excitation energy. For monomer separations smaller than 5 Å the distinction between Frenkel and CT excitations is less easy to make. All excitations are then of mixed Frenkel/CT nature, including some configurational mixing with the second-lowest molecular excitation. The complex evolution of the various excitation energies at intermolecular distances below 4 Å is due to extensive avoided crossing between the excited states and indicates a breakdown of the simple Frenkel exciton picture at such distances. The transition dipoles for the three lowest-lying excitations (calculated by integration over transition charge densities) are shown in Table 3, along with the monomer transition dipoles. The oscillator strength is concentrated in the transition to the second excited state, the “in-phase” exciton state; in this parallel geometry, the transition to the lower-energy “counter-phase” state has associated with it a net transition dipole moment of zero. We note that the third excitation gains oscillator strength at small displacements as it acquires some Frenkel character due to Frenkel/CT mixing. The low-lying excitations for the PY12 dimer show a qualitatively similar picture, and the interpretation in terms of Frenkel versus CT nature of the excitations is similar. The corresponding interaction energies, $\Delta E_{21} \equiv (E_2 - E_1)/2$, have been calculated for comparison with ΔE found from the excitonic model, i.e., using eq 1 or 3. The

**Figure 5.** (a) Exciton interaction energy ΔE for increasing vertical separation in the cyanine dimer, using ZINDO atomic transition charges, ab initio CIS atomic transition charges, and direct integration over the CIS transition charge density. (b) ΔE calculated for increasing vertical separation in the PY12 dimer, using the same approaches as in (a).

difference between ΔE_{21} from this “supermolecular” model and ΔE from the exciton model can then be taken as a measure of the validity of the exciton model. We may expect the exciton model to be more accurate as separation between monomers increases.

V. Discussion and Conclusions

Since it has been established that the point- and extended-dipole approximations are not adequate for our model dimers, we discuss first the relative accuracy of summation over atomic transition charges (eq 3) and integration over transition charge densities (eq 1) in evaluating ΔE . We note that the calculated exciton interaction energy has no well-defined sign, since the overall sign of the transition charge density can always be changed; in the results presented here we have consistently used the sign appropriate to the allowed transition (i.e., the in-phase combination of the monomeric excitations, as schematically indicated by the polarities shown in Figure 2, where the two colors of the poles indicate different signs of the transition density). In Figure 5a we compare ΔE for increasing vertical separation of the cyanine dimer, as evaluated using (Mulliken) atomic transition charges resulting from ZINDO, atomic transition charges from ab initio CIS, and direct integration over the CIS transition charge density. The summation over atomic transition charges gives results very similar to those of direct integration, generally differing only in the second or third decimal place for CIS. We see that differences are very small except at the smallest separations, below ~ 4 Å, where the interaction would be expected to be most sensitive to the details

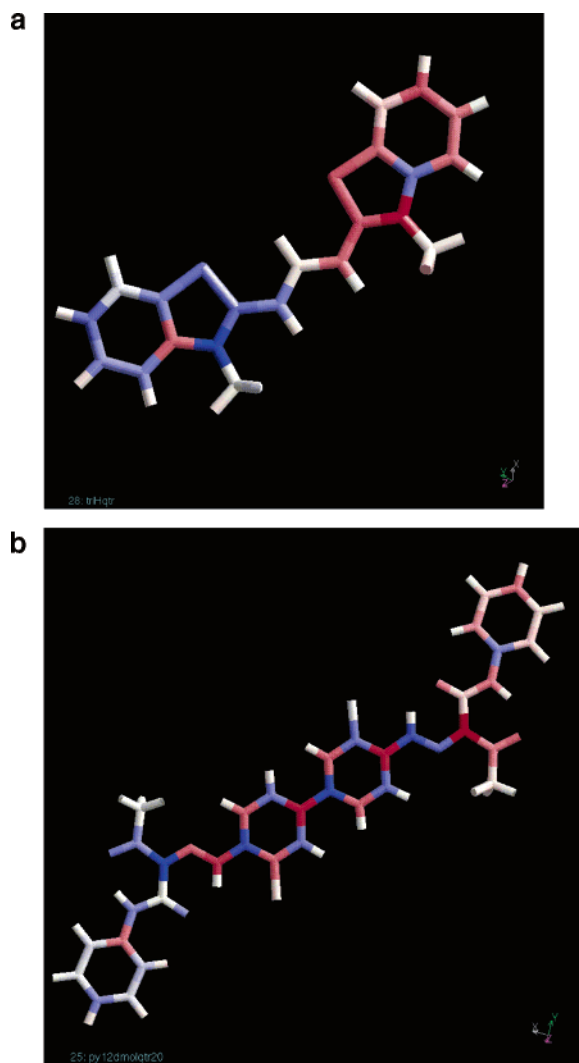


Figure 6. (a) ZINDO atomic transition charges plotted for the cyanine monomer; white denotes negligible charge. (b) ZINDO atomic transition charges for the PY12 monomer.

of transition charge distribution. Even then we find, for example, that at 3.6 Å separation, summation over ZINDO atomic transition charges gives 0.341 eV, ab initio CIS atomic transition charges give 0.323 eV, and integration over CIS transition charge densities gives 0.331 eV, so that transition charge summation gives values differing by only $\pm 2.7\%$ from the value due to integration. In Figure 5b the same comparison is made for the PY 12 dimer as a function of increasing vertical separation. It is clear that unless intermolecular distances are very small there is no significant advantage in evaluating the exciton interaction energy by integration from eq 1, as opposed to summing over atomic transition charges as per eq 3. Remarkably, there is no significant advantage either in using the ab initio level of calculation instead of the semiempirical level. The fact that the transition charge density distributions in the cyanine and in PY12 are of very different nature strongly suggests that these conclusions are quite generally valid. The transition charge density distribution in the cyanine molecule consists of well-separated positive and negative clouds (all atoms in each half of the molecule, with one exception, carry a transition charge of the same sign). ZINDO atomic transition charges for the cyanine monomer are shown in Figure 6a. This is not the case in the transition charge density distribution of the PY12 molecule, where the positive and negative transition charge clouds strongly interpenetrate, as indicated in the plot

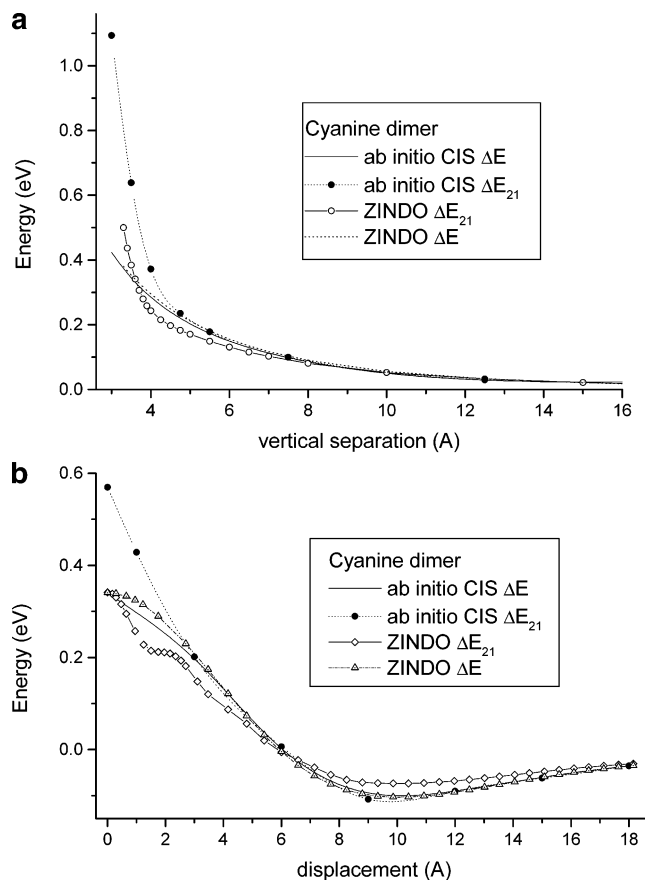


Figure 7. ΔE_{21} from the supermolecular model compared to ΔE from the exciton model, for two displacement paths, in the cyanine dimer. In (a), ΔE_{21} from ZINDO and from ab initio CIS are displayed along with ΔE from ZINDO atomic transition charges and from CIS integration, for vertical displacement. In (b), results for the longitudinal displacement path are shown.

of ZINDO atomic transition charges in Figure 6b. This also explains why the exciton shift in the cyanine dimer is substantially higher for identical separation than in the PY12 dimer. In the cyanine dimer the exciton interaction between parts of the transition charge clouds facing each other is almost exclusively destabilizing, while in the PY12 dimer it is composed of many destabilizing and stabilizing interactions between different fractions of the transition charge clouds, with the destabilizing ones slightly predominating.

We turn now to comparison of the exciton model and the supermolecular model. In Figure 7a, ΔE_{21} as defined in section IV and calculated from ZINDO and ab initio CIS is displayed along with ΔE from ZINDO transition charges and from ab initio CIS integration, for vertical displacement in the cyanine dimer. In Figure 7b the same quantities are shown for longitudinal displacement in the cyanine dimer. We note that while at large separation the interaction energies calculated using the supermolecular approach and the approaches of section III are very similar, at smaller separations they are not necessarily comparable. For separations less than ~ 4 Å, ZINDO results for ΔE_{21} are still comparable to—although not identical to— ΔE from the excitonic calculations, while ab initio CIS results give higher values by more than a factor of 2, corresponding to the expected CIS overestimate of excitation energies. Similar conclusions can be drawn from calculations on PY12 for both types of displacement; these are shown in Figure 8a,b. Data labeled “ZINDO ($E_2 - E_{mon}$)” in these figures do not represent the exciton shift, but rather the total shift of the allowed excitation in the dimer (i.e., including all interactions). This

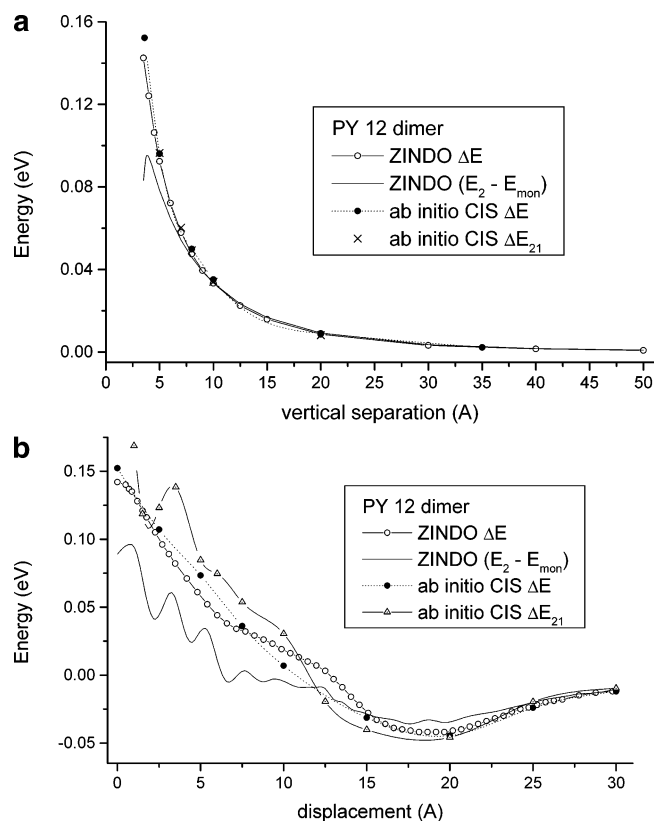


Figure 8. For PY12, ΔE from ZINDO atomic transition charges, and ΔE_{21} and ΔE (by integration) from ab initio CIS, for (a) vertical and (b) longitudinal displacement paths. The solid curves in (a) and (b) represent the difference between the (lowest) monomeric excitation energy E_{mon} and the excitation energy for the optically allowed dimer exciton state E_2 , as calculated with ZINDO.

provides an estimation at the semiempirical level of the relative size of the exciton interactions and the sum of the other contributions to the spectral shift. The differences in ΔE_{21} and ΔE can be attributed to several factors. First, and probably most importantly, as previously noted, the supermolecular model allows for charge-transfer excitation, while the excitonic model does not. Thus the deviation of the results for ΔE_{21} from ΔE can be taken as a measure of the importance of charge-transfer effects at small separations for this dimer. The close approach of the higher-lying dimer excited states to the second, for small separations, means that the excitonic energy splitting cannot be taken to be, as assumed in the excitonic model, purely a consequence of the energy difference of symmetric and anti-symmetric combinations of molecular states in which one monomer is in its first excited state and the other is not. The complex evolution of both the ZINDO and the ab initio CIS ΔE_{21} data as a function of the displacement, resembling an interference pattern, is caused by the fact that at this short vertical separation the interaction “feels” the detailed fine structure of the electron density and the transition charge density. It is obvious again that the simple Frenkel exciton model fails for such short intermolecular distances. However, the situation we studied here is a worst case. We have never seen perfect vertical stacking, as defined here, in real crystal structures. It is usually unfavorable because of steric and electrostatic repulsion. Nearest neighbors in aggregates or crystals are usually displaced laterally and/or longitudinally relative to a perfect vertical stacking, and one molecule is often inverted relative to the other. In such more realistic stackings we expect a smaller deviation from the Frenkel exciton model. For comparison, we plot in Figure 9 ΔE_{21} and ΔE for the cyanine from ab initio CIS, along

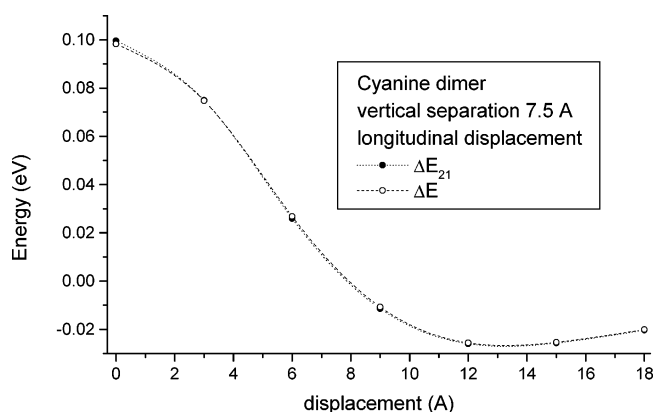


Figure 9. CIS-calculated values of ΔE_{21} and ΔE for the cyanine dimer, along the same longitudinal displacement path as in Figure 5b, but with a fixed vertical separation of 7.5 Å.

the same longitudinal displacement path as in Figure 7b, but with a fixed vertical separation of 7.5 Å between the monomers; as expected, the curves are now nearly coincident, with ΔE_{21} lying only marginally above ΔE at zero longitudinal displacement.

In conclusion, we have considered a range of approaches to calculation of the exciton interaction energy in a molecular solid, focusing on two model systems, a cyanine dimer and the PY 12 dimer. Neither the point-dipole or extended-dipole model is adequate for these systems; the point-dipole approximation in particular is completely inapplicable. However, summation over interaction between atomic transition charges gives a very good approximation to the values for the exciton interaction energy found by direct integration over transition charge densities. Furthermore, the agreement is not strongly dependent on the level of calculation or the method of transition charge partitioning, for the methods and cases considered; the semiempirical ZINDO approach is sufficiently accurate. The supermolecular model indicates that the exciton model is valid except at very small monomer separations.

Acknowledgment. I.A.H. acknowledges support from the IWT-Flemish region under grant no. IWT-161. The University of Antwerp is gratefully acknowledged for support under grant BOF UA/SFO UIA 2002.

References and Notes

- (1) Tiago, M. L.; Northrup, J. E.; Louie, S. G. *Phys. Rev. B* **2003**, *67*, 115212.
- (2) See, for example: Davydov, A. S. *Theory of Molecular Excitons*; Plenum: New York, 1971.
- (3) Kelley, A.; Myers, J. *Chem. Phys.* **2003**, *119*, 3320.
- (4) Champagne, B.; Bishop, D. M. *Adv. Chem. Phys.* **2003**, *126*, 41.
- (5) Ecoffet, C.; Markovitsi, D.; Millié, P.; Lemaître, J.-P. *Chem. Phys.* **1993**, *177*, 629.
- (6) Baraldi, I.; Momicchioli, F.; Ponterini, G.; Tatikolov, A. S.; Vanossi, D. *J. Phys. Chem. A* **2001**, *105*, 4600.
- (7) Zimmermann, J.; Siggel, U.; Fuhrhop, J.-H.; Röder, B. *J. Phys. Chem. B* **2003**, *107*, 6020.
- (8) Scholes, G. D.; Ghiggino, K. P. *J. Phys. Chem.* **1994**, *98*, 4580.
- (9) Scholz, R.; Vragovic, I.; Kobitski, A. Yu.; Salvan, G.; Kampen, T. U.; Schreiber, M.; Zahn, D. R. T. *Proc. Int. Sch. Phys. “Enrico Fermi”* **2002**, *149* (Organic Nanostructures: Science and Applications), 379.
- (10) Mazur, G.; Petelenz, P.; Slawik, M. *J. Chem. Phys.* **2003**, *118*, 1423.
- (11) Beljonne, D.; Cornil, J.; Silbey, R.; Millié, P.; Brédas, J. L. *J. Chem. Phys.* **2000**, *112*, 4749.
- (12) Beenken, W. J. D.; Pullerits, T. *J. Chem. Phys.* **2004**, *120*, 2490.
- (13) Delley, B. *J. Chem. Phys.* **1990**, *92*, 508.
- (14) Bacon, A. D.; Zerner, M. C. *Theor. Chim. Acta* **1979**, *53*, 21.
- (15) Van Alsenoy, C.; Peeters, A. *J. Mol. Struct. (THEOCHEM)* **1993**, *286*, 19.

- (16) Kasha, M.; Rawls, H. R.; El-Bayoumi, M. A. *Pure Appl. Chem.* **1965**, *11*, 371.
- (17) Czikkely, V.; Försterling, H. D.; Kuhn, H. *Chem. Phys. Lett.* **1970**, *6*, 207.
- (18) Scholes, G. D. In *Resonance Energy Transfer*; Wiley: New York, 1998.
- (19) Norland, K.; Ames, A.; Taylor, T. *Photogr. Sci. Eng.* **1970**, *14*, 295.
- (20) Würther, F.; Yao, S.; Debaerdemaeker, T.; Wortman, R. *J. Am. Chem. Soc.* **2002**, *124*, 9431.
- (21) Endo, A.; Matsumoto, S.; Mizuguchi, J. *J. Phys. Chem. A* **1999**, *103*, 8193.
- (22) Hwang, I.-W.; Cho, H. S.; Jeong, D. H.; Kim, D.; Tsuda, A.; Nakamura, T.; Osuka, A. *J. Phys. Chem. B* **2003**, *107*, 9977.
- (23) Mulliken, R. S. *J. Chem. Phys.* **1955**, *23*, 1833.
- (24) Hirshfeld, F. L. *Theor. Chim. Acta* **1977**, *44*, 129. Rousseau, B.; Peeters, A.; Van Alsenoy, C. *Chem. Phys. Lett.* **2000**, *324*, 189.
- (25) Millié, P.; Momicchioli, F.; Vanossi, D. *J. Phys. Chem. B* **2000**, *104*, 9621.
- (26) Cornil, J.; dos Santos, D. A.; Crispio, X.; Silbey, R.; Brédas, J. L. *J. Am. Chem. Soc.* **1998**, *120*, 1289.
- (27) Baraldi, I.; Caselli, M.; Momicchioli, F.; Ponterini, G.; Vanossi, D. *Chem. Phys.* **2002**, *275*, 149.